

Electronic Supplementary Information for

**Modulation of magnetization dynamics of an Er(III)
coordination polymer by the conversion of a ligand to a radical
using UV light**

Xiaoshuang Gou, Ning Liu, Yuewei Wu, Wenlong Lan, Mengmeng Wang, Wei Shi* and Peng Cheng*

Department of Chemistry, Key Laboratory of Advanced Energy Materials Chemistry
(MOE) and Frontiers Science Center for New Organic Matter, College of Chemistry,
Nankai University, Tianjin 300071, China.

Table of Contents

1. Experimental section.....	S2
2. Figures.....	S5
3. Tables.....	S38
4. References.....	S45

Experimental section

Materials. Chemicals and solvents were purchased from commercial vendors and used as received without further purification. 2,5-Dichloro-3,6-dihydroxy-p-quinone (H₂CA, 98%, Tokyo Chemical Industry Development Co., LTD), Erbium chloride hexahydrate (ErCl₃·6H₂O, 99.99%, Sigma-Aldrich Trading Co., LTD), 9-Anthracenecarboxylic acid (HACA, 98%, Bide Pharmatech LTD.), N,N-Dimethylformamide (DMF, AR, Tianjin Concord Technology Co. LTD).

Physical measurements. Elemental analyses (EA) for H, C and N were executed on a Vario EL CUBE elemental analyzer. Fourier transform infrared (FT-IR) spectra were performed in the range 400–4000 cm⁻¹ on a Bruker ALPHA FT-IR spectrophotometer equipped with an attenuated total reflectance accessory. Powder X-ray diffraction (PXRD) measurements were performed on a Rigaku Smartlab SE X-ray diffractometer using Mo-K α radiation. Thermogravimetric analyses (TGA) were carried out on a Mettler Toledo TGA 2 thermal analyzer in the range 40–800 °C (heating rate = 5 °C/min) under N₂ atmosphere. UV-vis absorption spectra were measured by a Shimadzu UV-2600 spectrophotometer. Electron paramagnetic resonance (EPR) spectra were respectively collected at room temperature using a Bruker E580-10/12 EPR spectrometer. Static (direct current, dc) magnetic susceptibility measurements were recorded on a Quantum Design SQUID (MPMS) VSM magnetometer and corrected by the sample holder contribution and diamagnetic contributions estimated using Pascal's constants.^[1] Dynamic (alternating

current, ac) magnetic susceptibilities were measured on a Quantum Design SQUID (MPMS) VSM or a PPMS magnetometer.

Synthesis of $[Er(CA)(ACA)(DMF)(H_2O)]_n$ (1). ErCl₃·6H₂O (0.1 mmol, 38.1 mg), H₂CA (0.02 mmol, 4.2 mg), HACA (0.04 mmol, 8.9 mg), DMF (5.2 mL) and H₂O (8 mL) were added into a 20 mL glass vial. The mixture was ultrasonicated for about ten minutes to be completely dissolved. The glass vial was heated at 96 °C for 9.5 hours. After cooling down to room temperature, rhomboid shaped brown crystals were collected, washed by water (5 mL × 5), and dried under air. Yield: 54.3% based on H₂CA. Anal. Calcd for C₂₄H₁₈Cl₂NO₈Er: C, 41.97; H, 2.64; N, 2.04. Found (1): C, 41.52; H, 2.69; N, 2.27. Found (1a): C, 41.58; H, 2.62; N, 2.05. FT-IR (ATR, cm⁻¹): 3574 (w), 1664 (m), 1625 (w), 1576 (m), 1495 (s), 1454 (w), 1433 (w), 1376 (s), 1325 (w), 1293 (w), 1279 (w), 1112 (m), 1063 (w), 1005 (m), 883 (w), 871 (w), 848 (s), 791 (w), 774 (w), 731 (m), 682 (m), 674 (m), 649 (m), 605 (m), 576 (s), 560 (w), 465 (s), 449 (m), 408 (m).

Synthesis of $[Er_{0.17}Y_{0.83}(CA)(ACA)(DMF)(H_2O)]_n$ (1@Y). 1@Y was prepared by the same synthetic procedure as 1 with ErCl₃·6H₂O and YCl₃·6H₂O in a 1:7 molar ratio. ICP: Er/Y = 1 : 4.97. Anal. Calcd for C₂₄H₁₈Cl₂NO₈Er_{0.17}Y_{0.83}: C, 46.37; H, 2.91; N, 2.25. Found (1@Y): C, 46.30; H, 2.96; N, 2.17. Found (1a@Y): C, 46.43; H, 2.93; N, 2.24. FT-IR (ATR, cm⁻¹): 3570(w), 1666 (m), 1625 (w), 1580 (m), 1497 (s), 1454 (w), 1434 (w), 1376 (s), 1324 (w), 1295 (w), 1279 (w), 1112 (m), 1063 (w), 1005 (m), 884 (w), 871 (w), 848 (s), 791 (w), 775 (w), 733 (m), 684 (m), 674 (m), 651 (m), 604 (m), 578 (s), 560 (w), 463 (s), 449 (m), 408 (m).

X-ray Structure Determination. Single crystal of **1** suitable for X-ray analysis was coated with Parabar oil and mounted on a MicroMounts rod. The crystallographic data were collected at 298(2) K on a Rigaku XtaLAB Mini II single-crystal diffractometer using graphite-monochromatic Mo-K α radiation ($\lambda = 0.71073 \text{ \AA}$). The structure of **1** was solved by the direct methods with SHELXS and refined based on full-matrix least-squares techniques against F^2 using the program package Olex2 version 1.5.^[2] The disordered O atoms in the structure were treated by split or occupancies refinement. All non-hydrogen atoms were refined with anisotropic displacement parameters during the final cycles while the hydrogen atoms of the ligands were generated in ideal positions with isotropic displacement parameters. The parameters, data collection, and refinements of **1** are summarized in [Table S1](#). The asymmetric unit of **1** displaying atomic displacement parameters (ADPs) was shown in Fig. S33. Detailed crystallographic information can be obtained from the CCDC database under the deposition number 2165479.

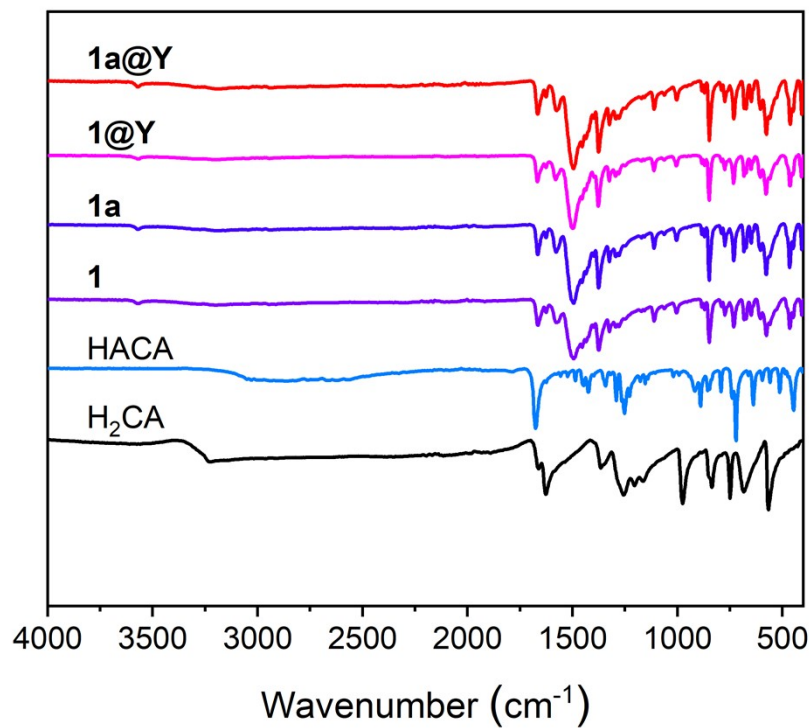


Fig. S1 IR spectra for H₂CA, HACA, **1**, **1a**, **1@Y** and **1a@Y**.

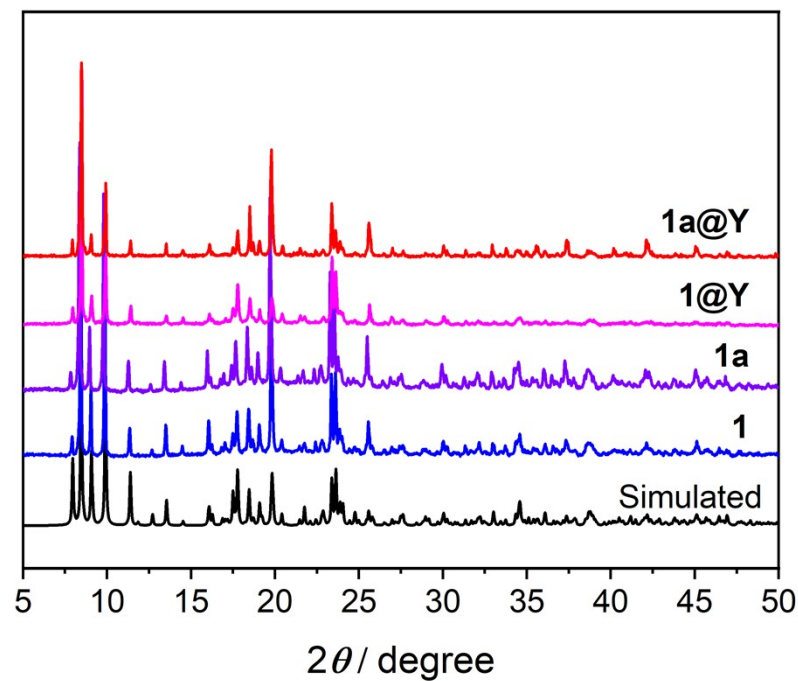


Fig. S2 Experimental and simulated PXRD patterns for **1**, **1a**, **1@Y** and **1a@Y**.

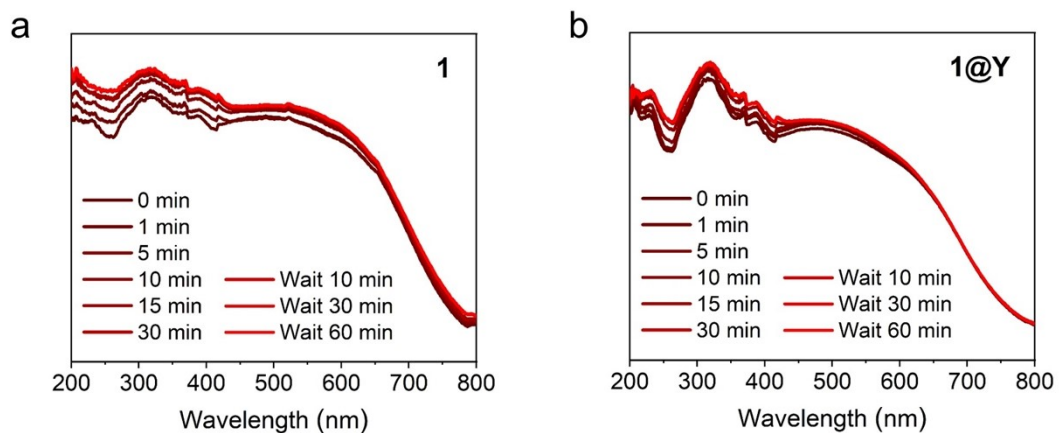


Fig. S3 Time-dependent UV-vis spectra of **1** (a) and **1@Y** (b) upon light irradiation.

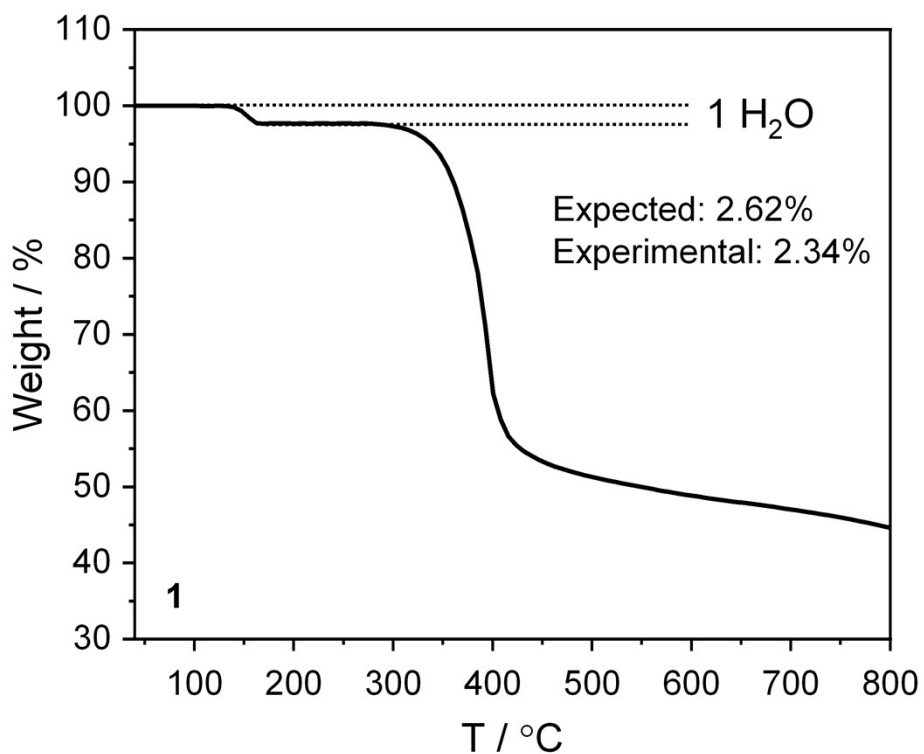


Fig. S4 Thermogravimetric analysis of **1** under N₂ atmosphere (heating rate = 5 °C/min).

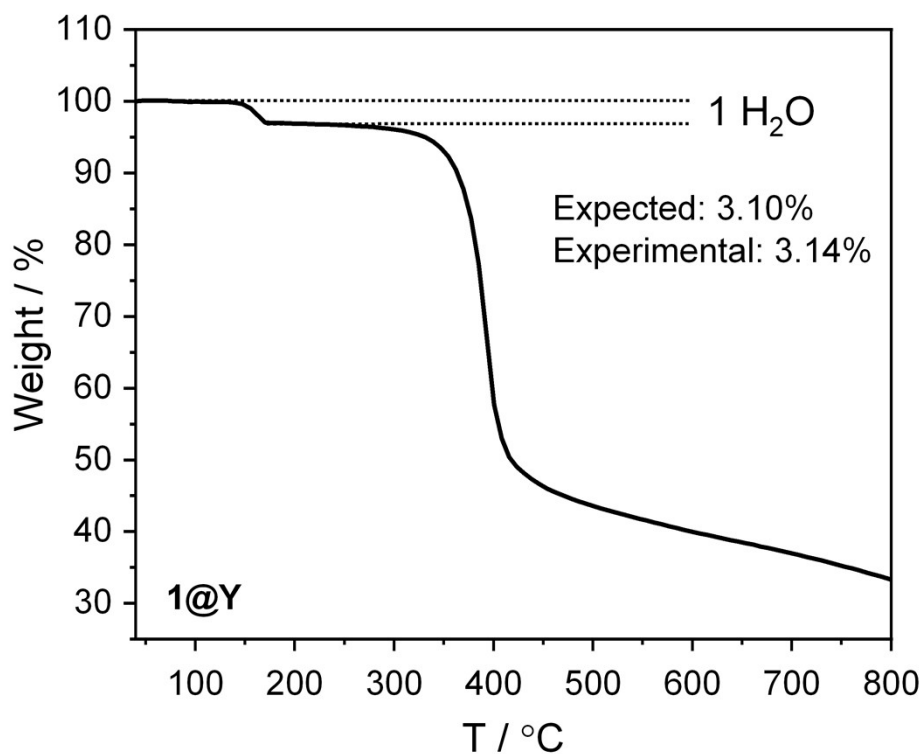


Fig. S5 Thermogravimetric analysis of **1@Y** under N₂ atmosphere (heating rate = 5 °C/min).

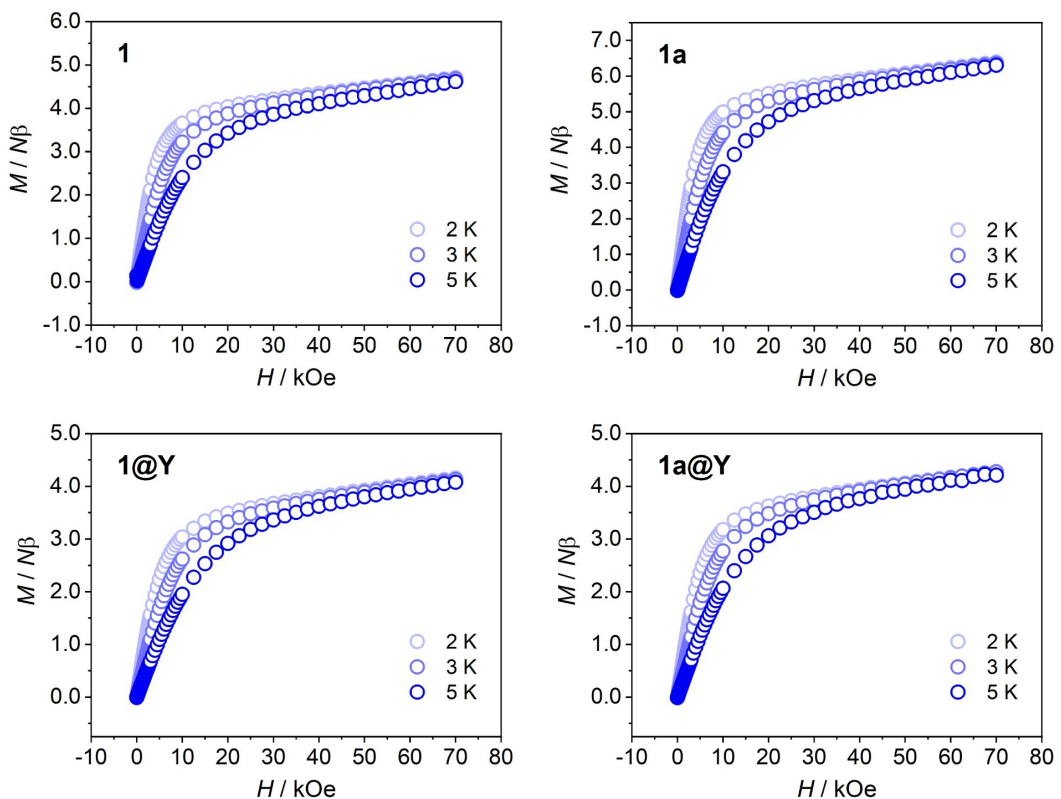


Fig. S6 Variable field magnetizations of **1**, **1a**, **1@Y** and **1a@Y** at 2, 3 and 5 K.

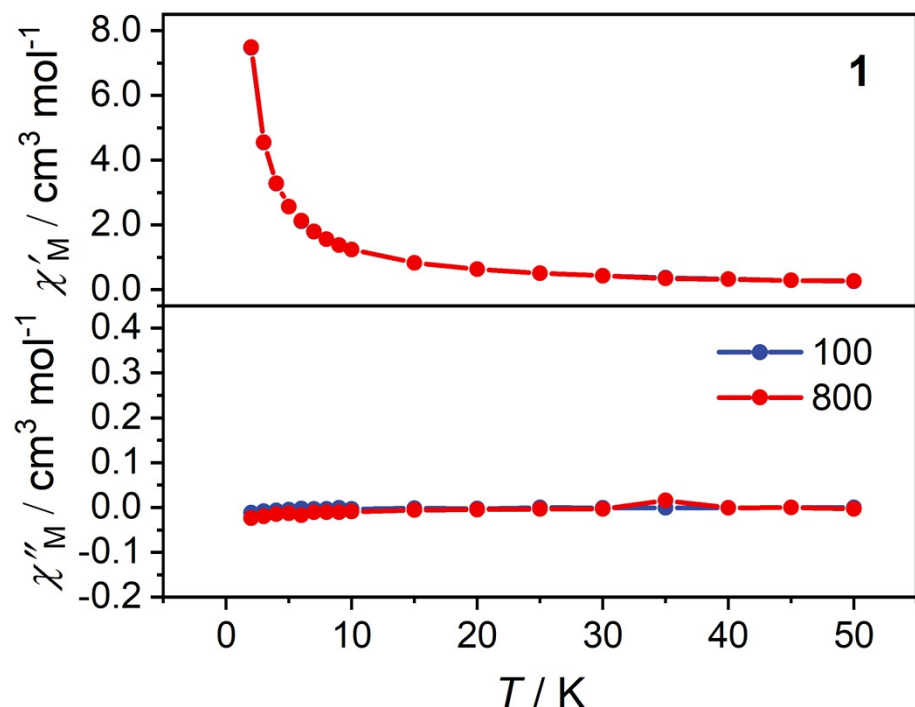


Fig. S7 Temperature dependence of the χ' and χ'' for **1**, collected in zero dc field in the temperature range of 2–50 K, $\nu = 100, 800$ Hz.

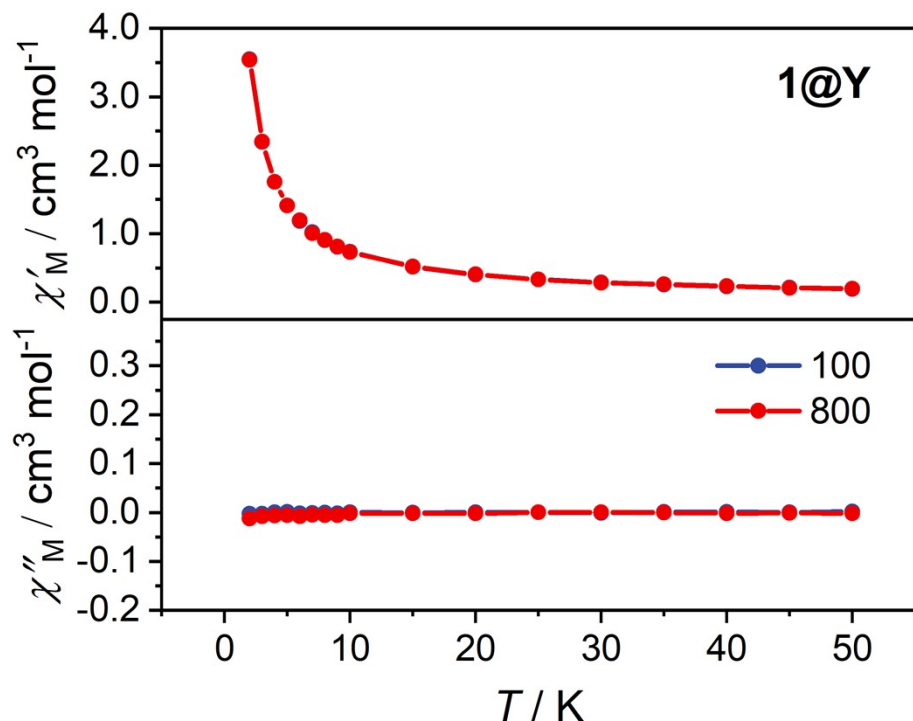


Fig. S8 Temperature dependence of the χ' and χ'' for **1@Y**, collected in zero dc field in the temperature range of 2–50 K, $\nu = 100, 800$ Hz.

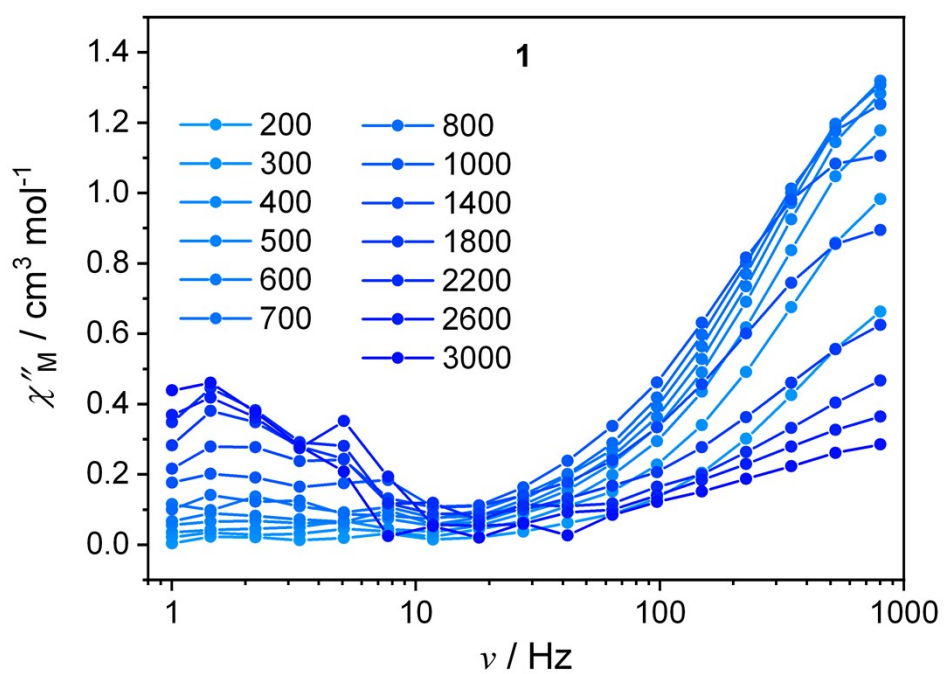


Fig. S9 Frequency dependence of the χ'' at 2 K in various dc fields for **1**.

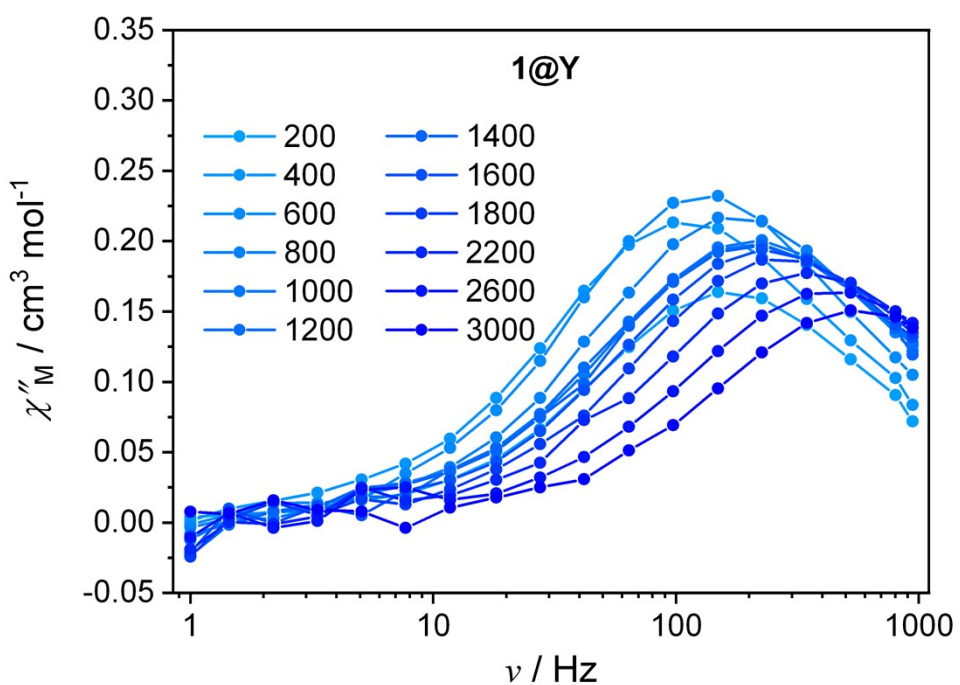


Fig. S10 Frequency dependence of the χ'' at 2 K in various dc fields for **1@Y**.

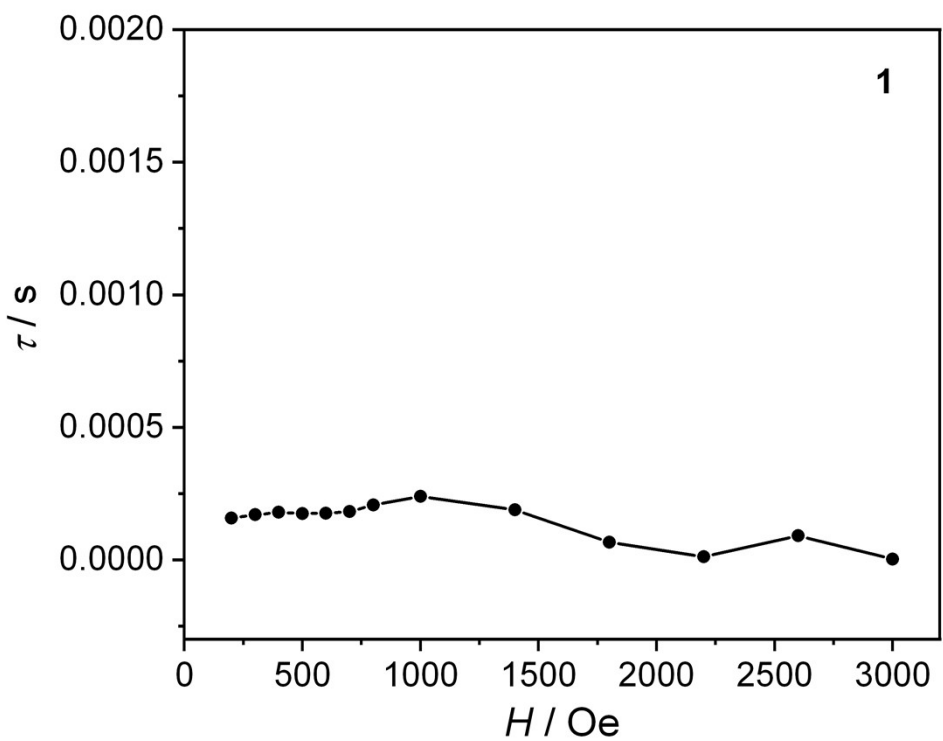


Fig. S11 Field dependence of the magnetic relaxation time (τ) for **1**.

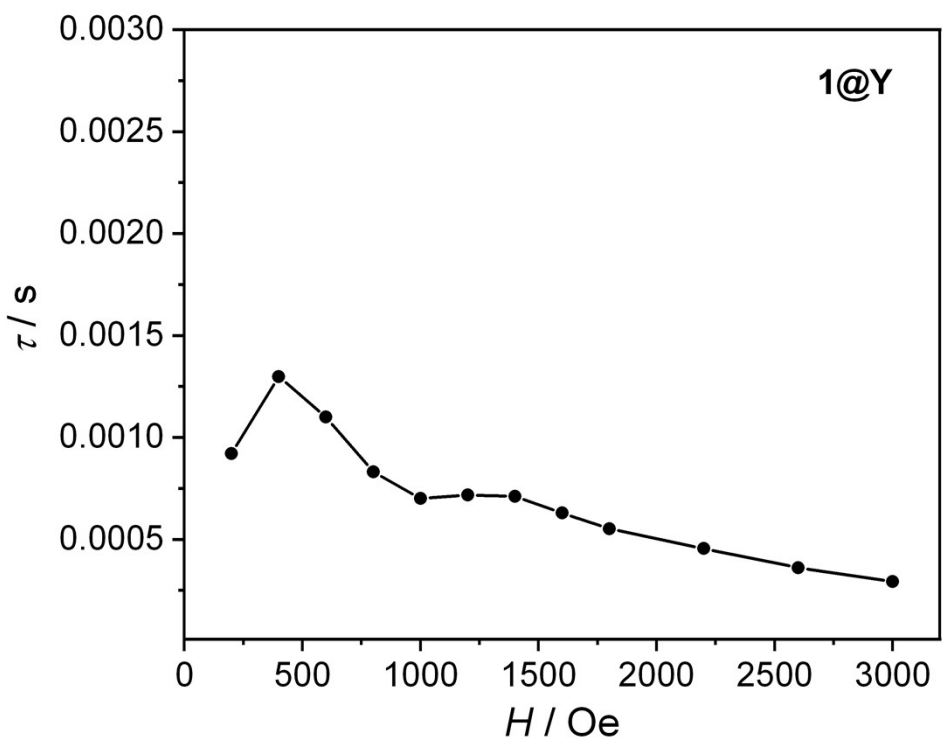


Fig. S12 Field dependence of the magnetic relaxation time (τ) for **1@Y**.

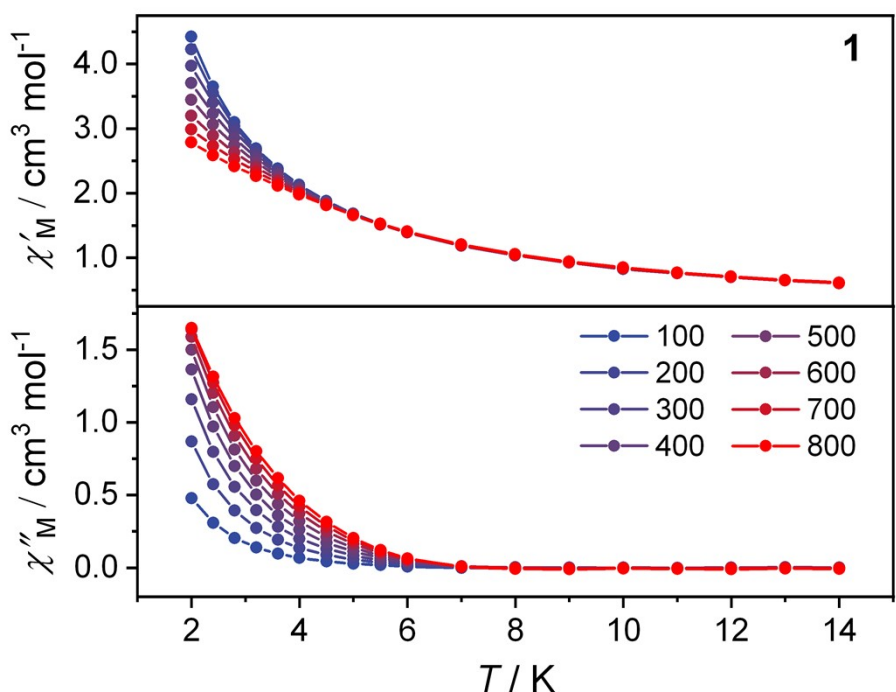


Fig. S13 Temperature dependence of the in-phase χ' and out-of-phase χ'' molar magnetic susceptibility for **1**, collected in 600 Oe dc field in the temperature range of 2–14 K, ν = 100–800 Hz.

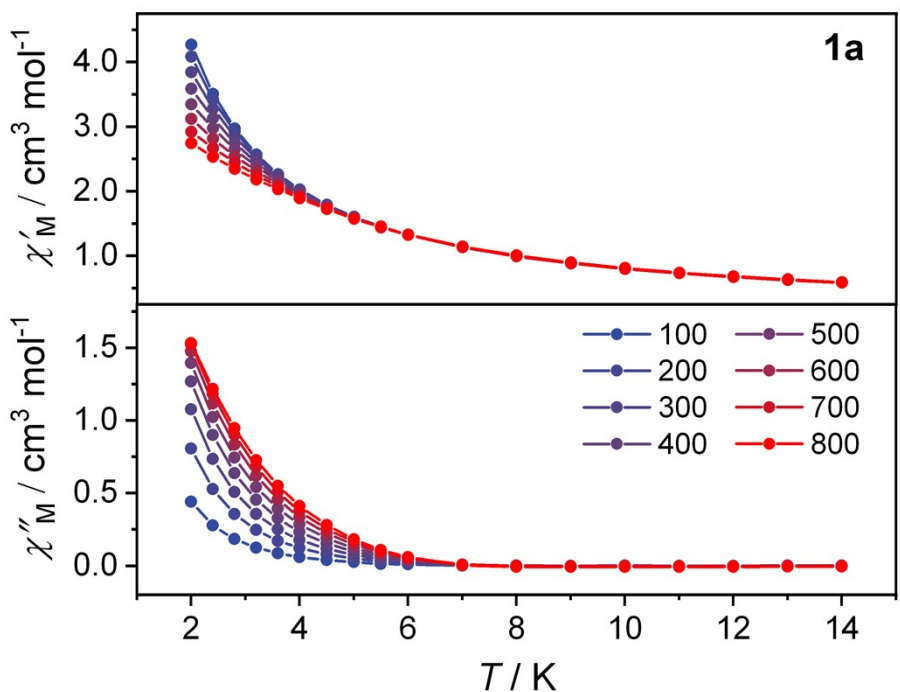


Fig. S14 Temperature dependence of the in-phase χ' and out-of-phase χ'' molar magnetic susceptibility for **1a**, collected in 600 Oe dc field in the temperature range of 2–14 K, $\nu = 100\text{--}800$ Hz.

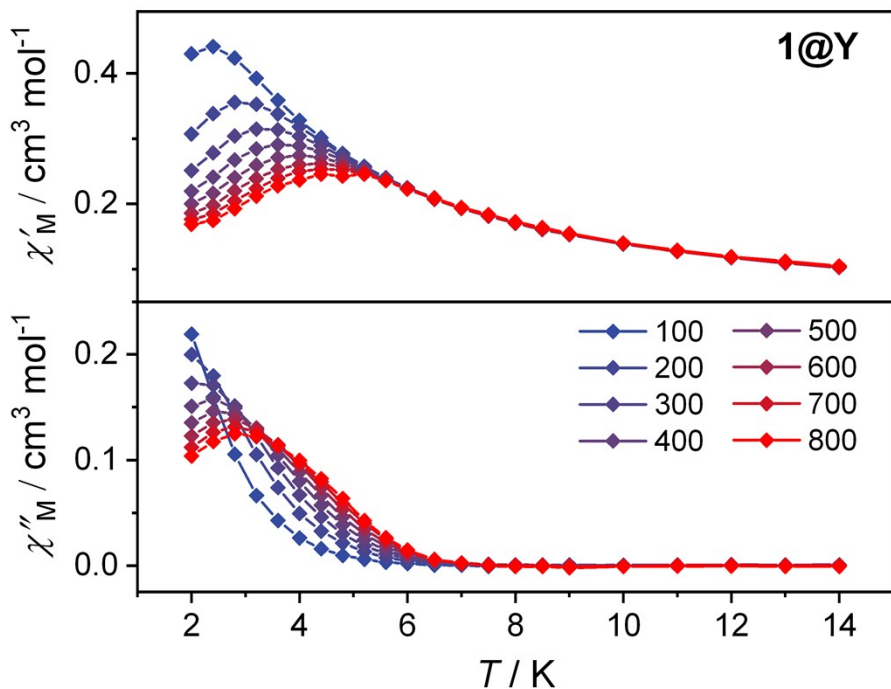


Fig. S15 Temperature dependence of the in-phase χ' and out-of-phase χ'' molar magnetic susceptibility for **1@Y**, collected in 400 Oe dc field in the temperature range of 2–14 K, $\nu = 100\text{--}800$ Hz.

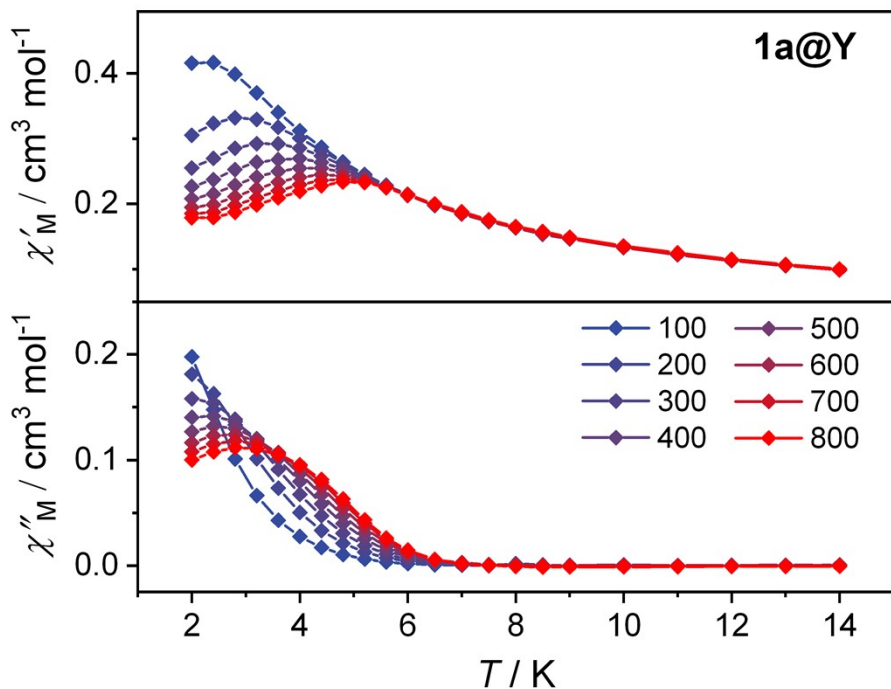


Fig. S16 Temperature dependence of the in-phase χ' and out-of-phase χ'' molar magnetic susceptibility for **1a@Y**, collected in 400 Oe dc field in the temperature range of 2–14 K, $\nu = 100\text{--}800$ Hz.

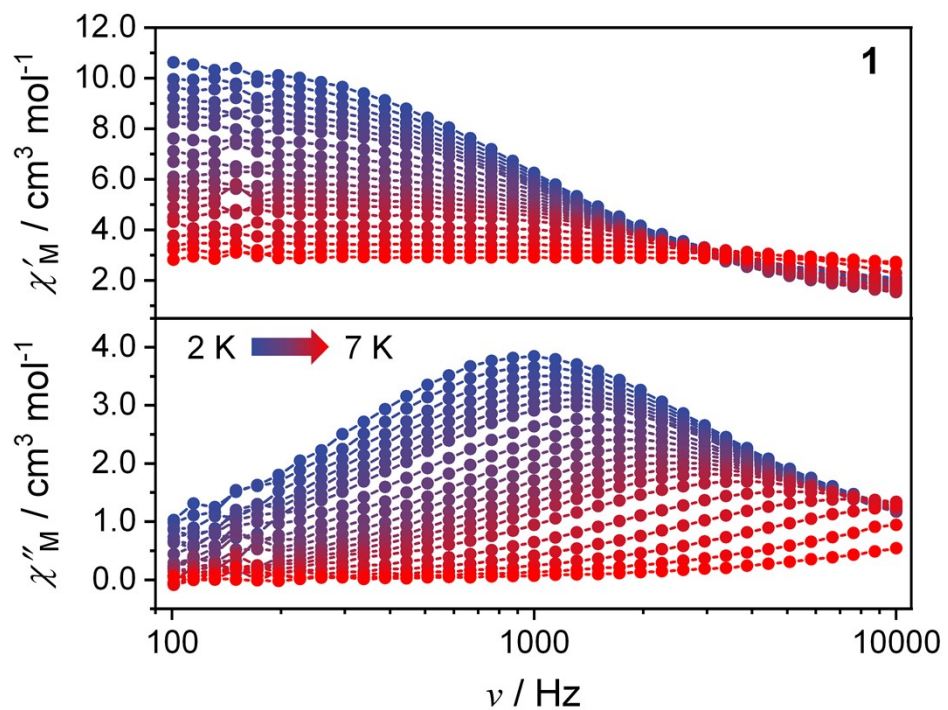


Fig. S17 Frequency dependence of the in-phase χ' and out-of-phase χ'' molar magnetic susceptibility for **1**, collected in 600 Oe dc field at ac frequencies of $\nu = 100$ to 10000 Hz (PPMS).

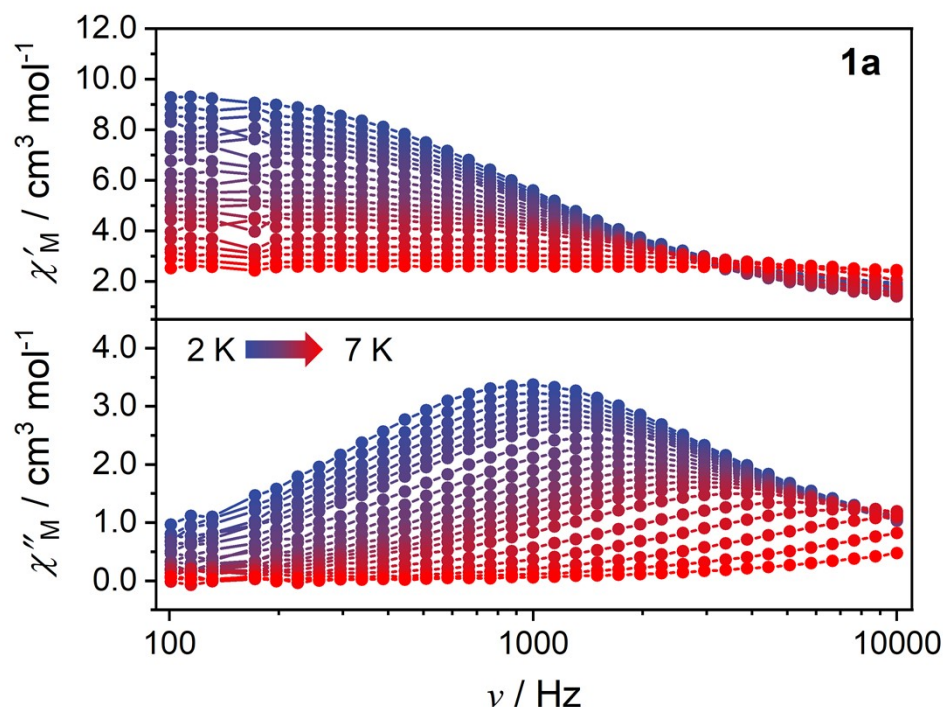


Fig. S18 Frequency dependence of the in-phase χ' and out-of-phase χ'' molar magnetic susceptibility for **1a**, collected in 600 Oe dc field at ac frequencies of $\nu = 100$ to 10000 Hz (PPMS).

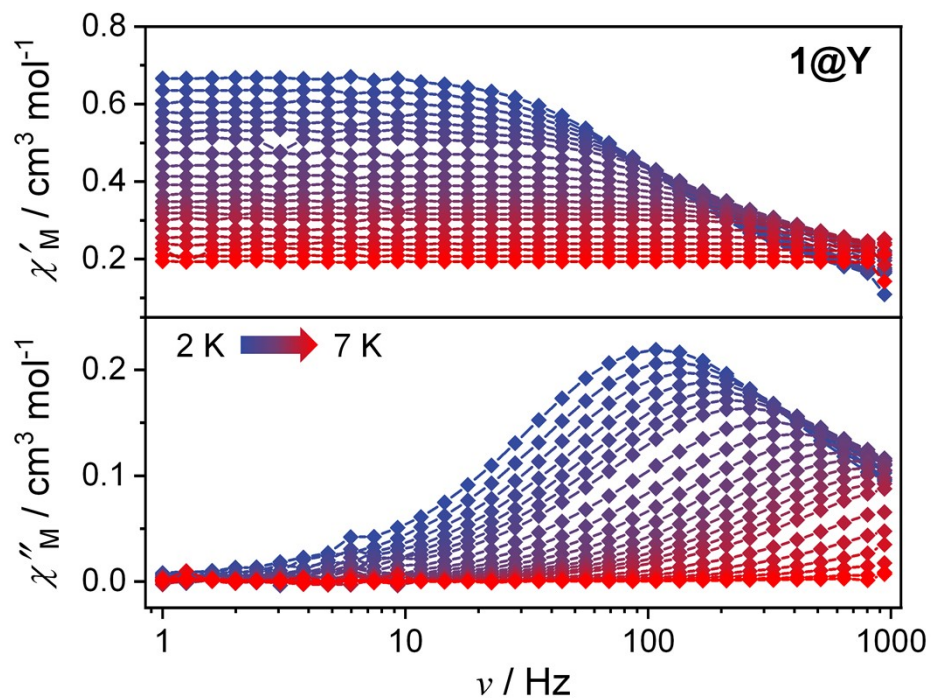


Fig. S19 Frequency dependence of the in-phase χ' and out-of-phase χ'' molar magnetic susceptibility for **1@Y**, collected in 400 Oe dc field at ac frequencies of $\nu = 1$ to 1000 Hz (MPMS).

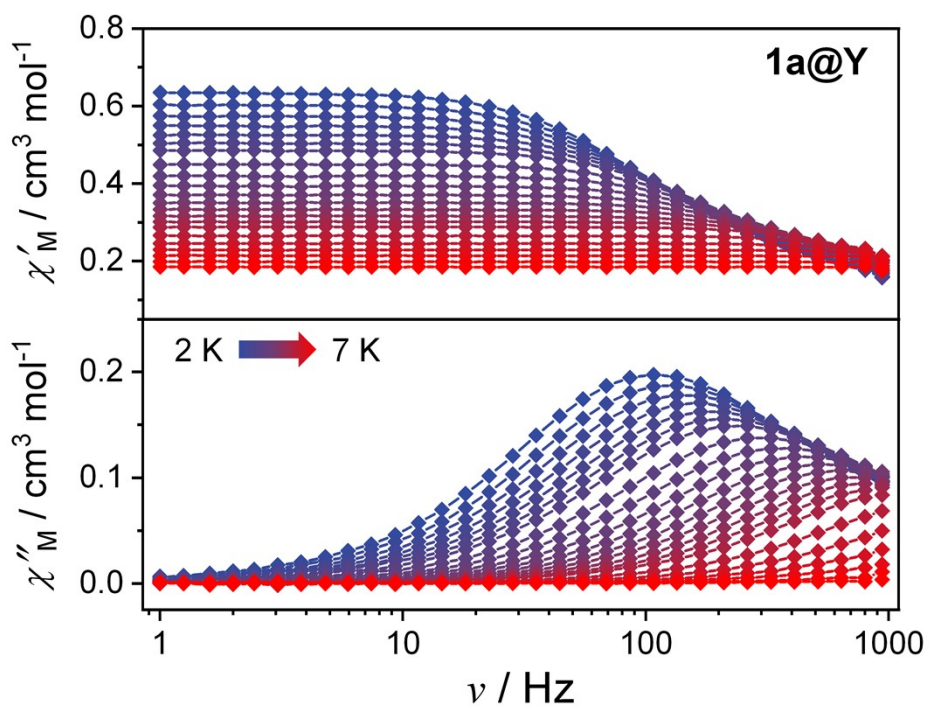


Fig. S20 Frequency dependence of the in-phase χ' and out-of-phase χ'' molar magnetic susceptibility for **1a@Y**, collected in 400 Oe dc field at ac frequencies of $\nu = 1$ to 1000 Hz (MPMS).

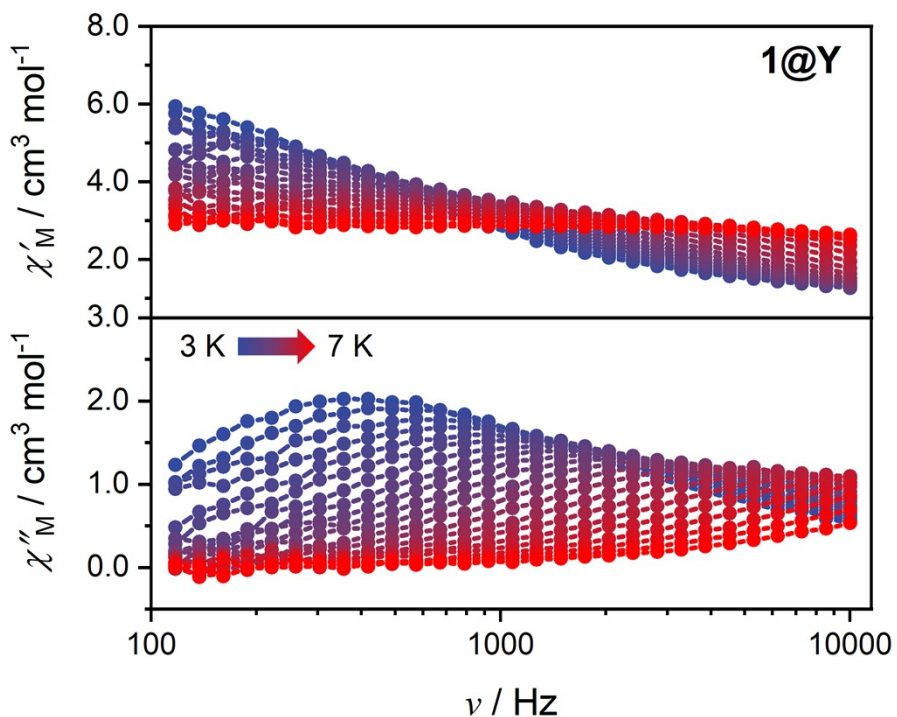


Fig. S21 Frequency dependence of the in-phase χ' and out-of-phase χ'' molar magnetic susceptibility for **1@Y**, collected in 400 Oe dc field at ac frequencies of $\nu = 100$ to 10000 Hz (PPMS).

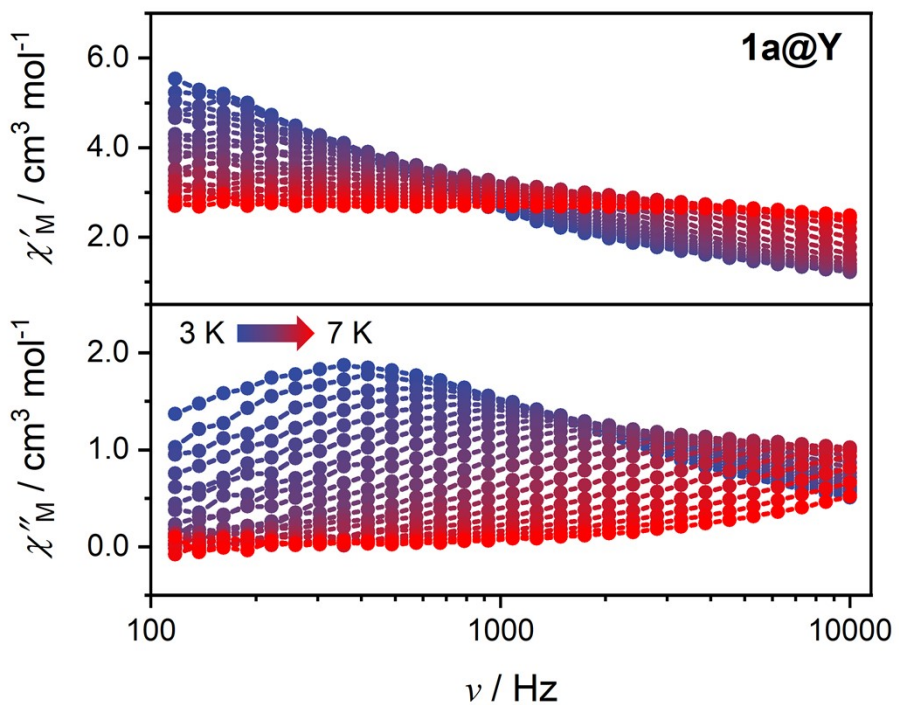


Fig. S22 Frequency dependence of the in-phase χ' and out-of-phase χ'' molar magnetic susceptibility for **1a@Y**, collected in 400 Oe dc field at ac frequencies of $\nu = 100$ to 10000 Hz (PPMS).

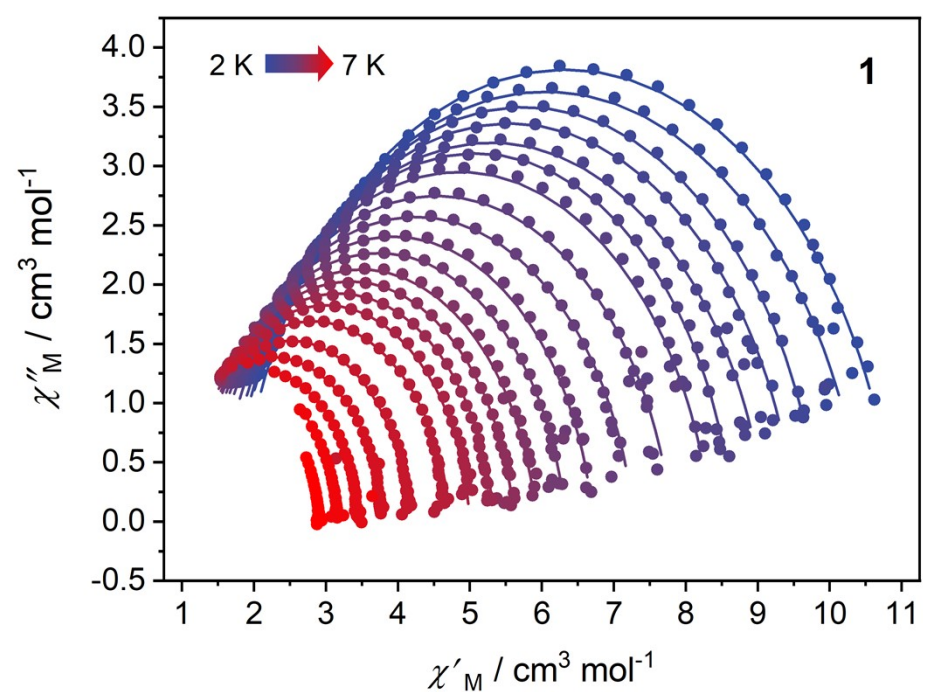


Fig. S23 Cole-Cole plots for **1**. $\alpha = 0.04\text{--}0.17$ (PPMS).

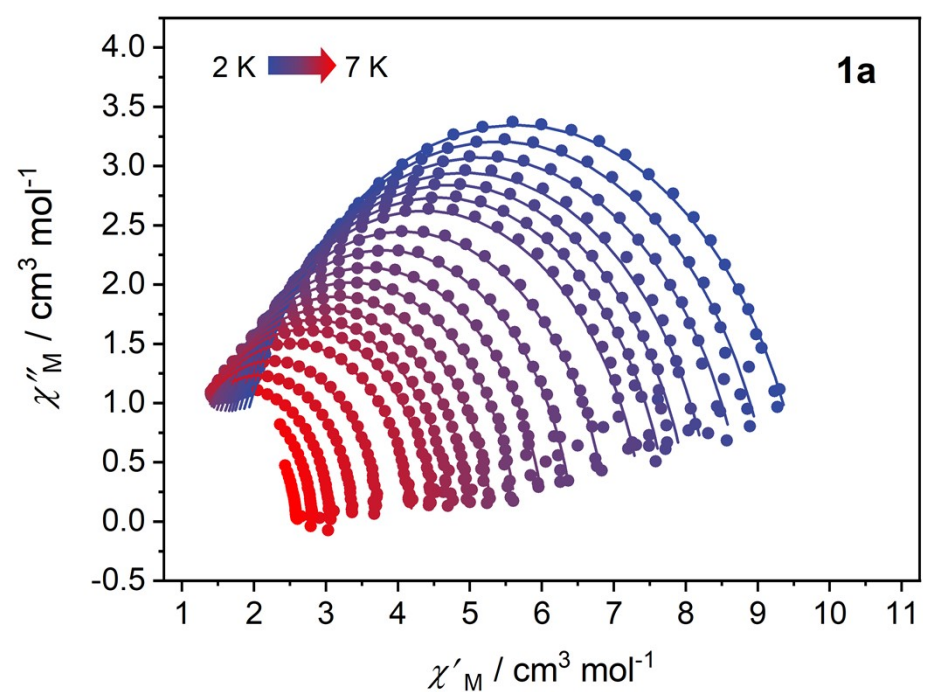


Fig. S24 Cole-Cole plots for **1**. $\alpha = 0.02\text{--}0.12$ (PPMS).

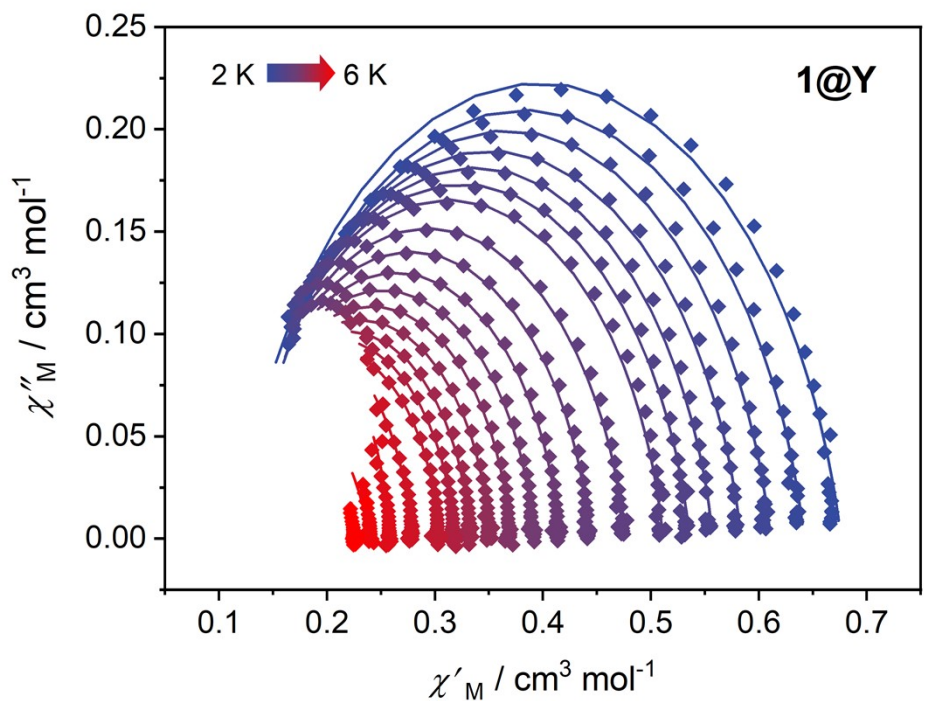


Fig. S25 Cole-Cole plots for **1**. $\alpha = 0.05\text{--}0.21$ (MPMS).

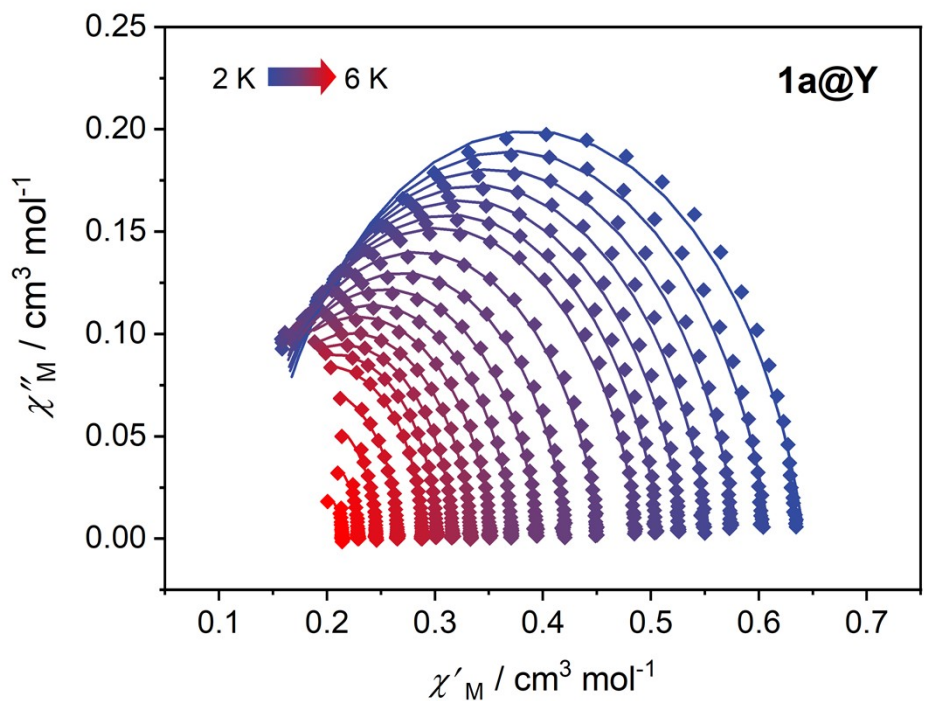


Fig. S26 Cole-Cole plots for **1a@Y**. $\alpha = 0\text{--}0.15$ (MPMS).

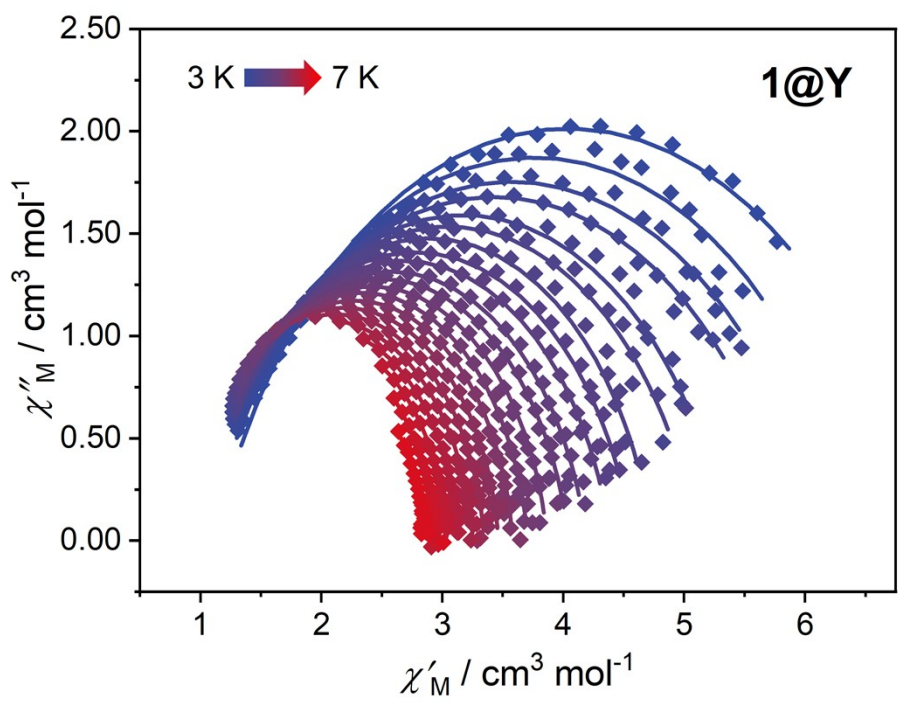


Fig. S27 Cole-Cole plots for **1**. $\alpha = 0.05\text{--}0.24$ (PPMS).

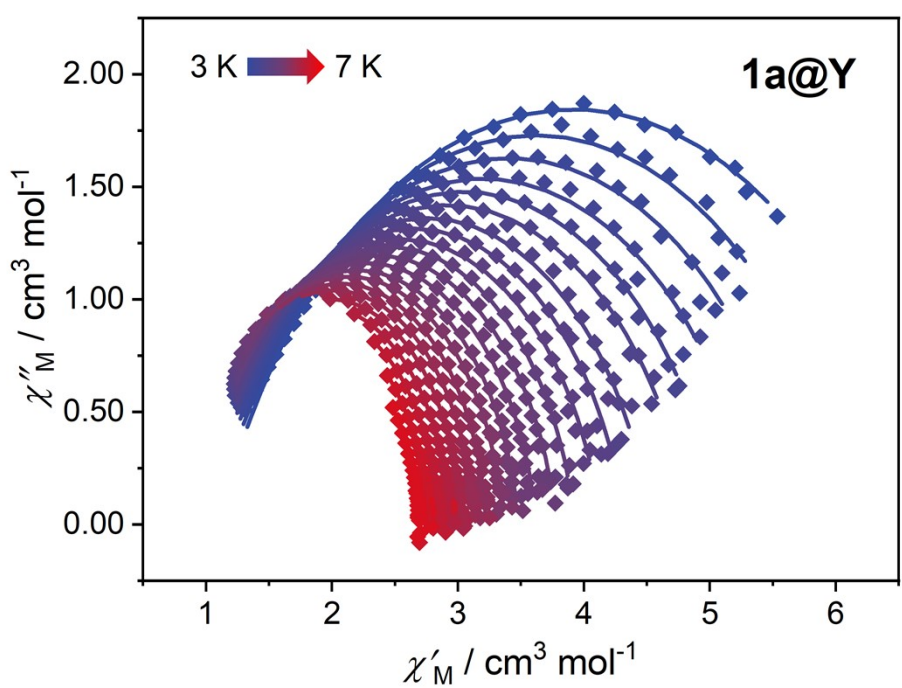


Fig. S28 Cole-Cole plots for **1a@Y**. $\alpha = 0.03\text{--}0.26$ (PPMS).

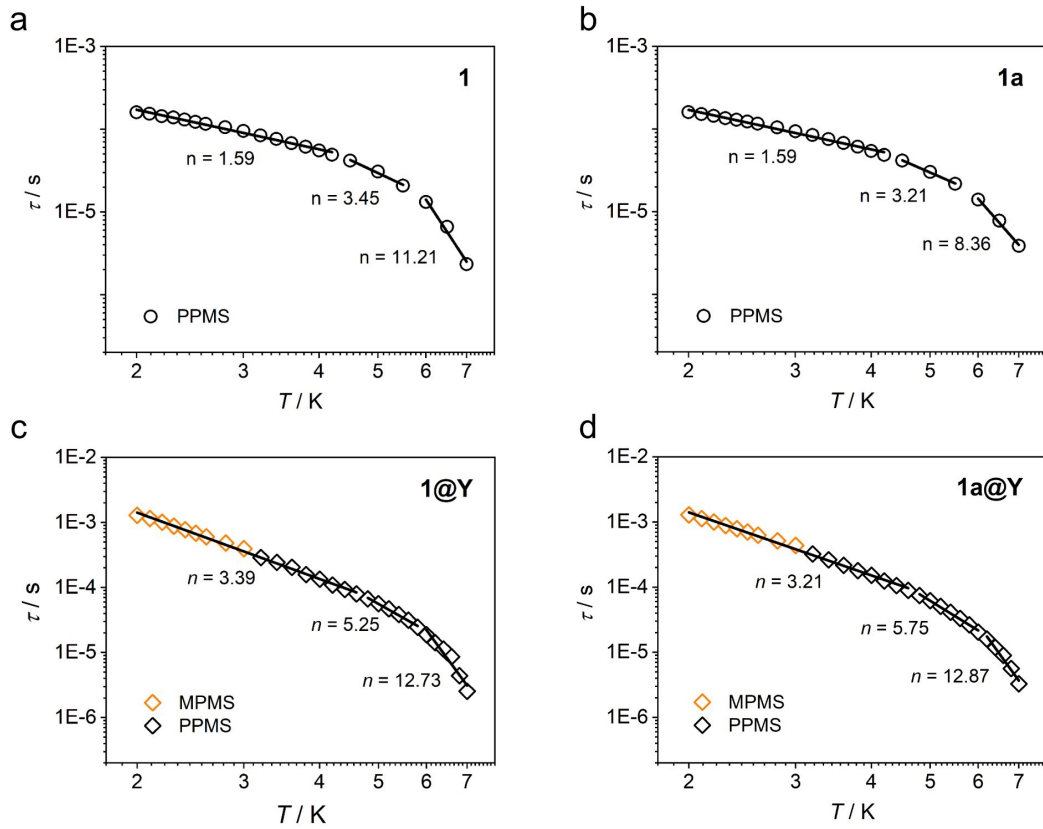


Fig. S29 The plots of the relaxation time τ vs T on a log-log scale for **1**, **1a**, **1@Y** and **1a@Y**.

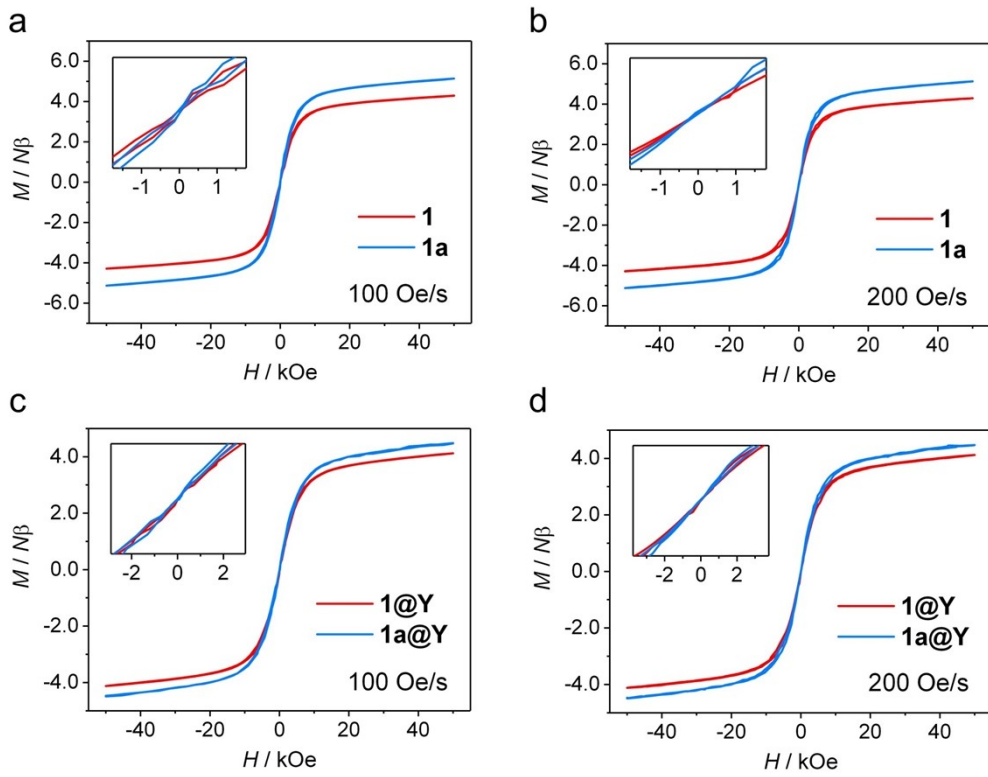


Fig. S30 Magnetic hysteresis loops of **1**, **1a** (a, b), **1@Y** and **1a@Y** (c, d) at 2 K with field sweep rates of 100 and 200 Oe s⁻¹.

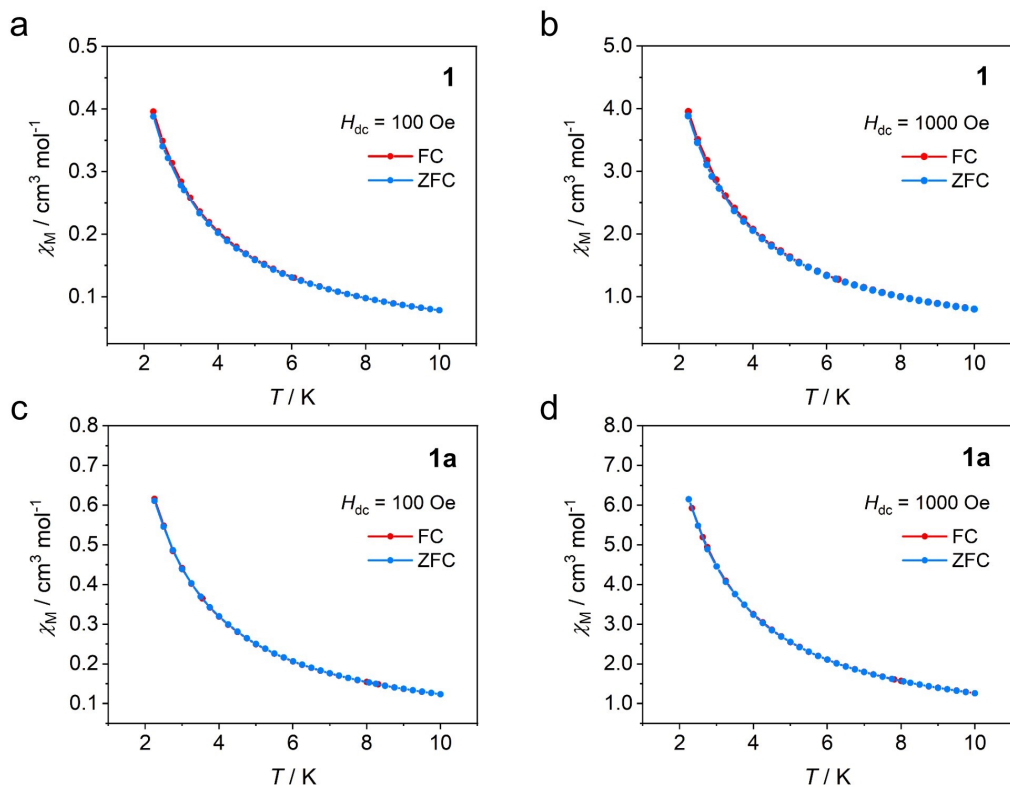


Fig. S31 FC/ZFC magnetizations at 100 Oe and 1000 Oe for **1** (a, b) and **1a** (c, d). The lines are guides for the eye.

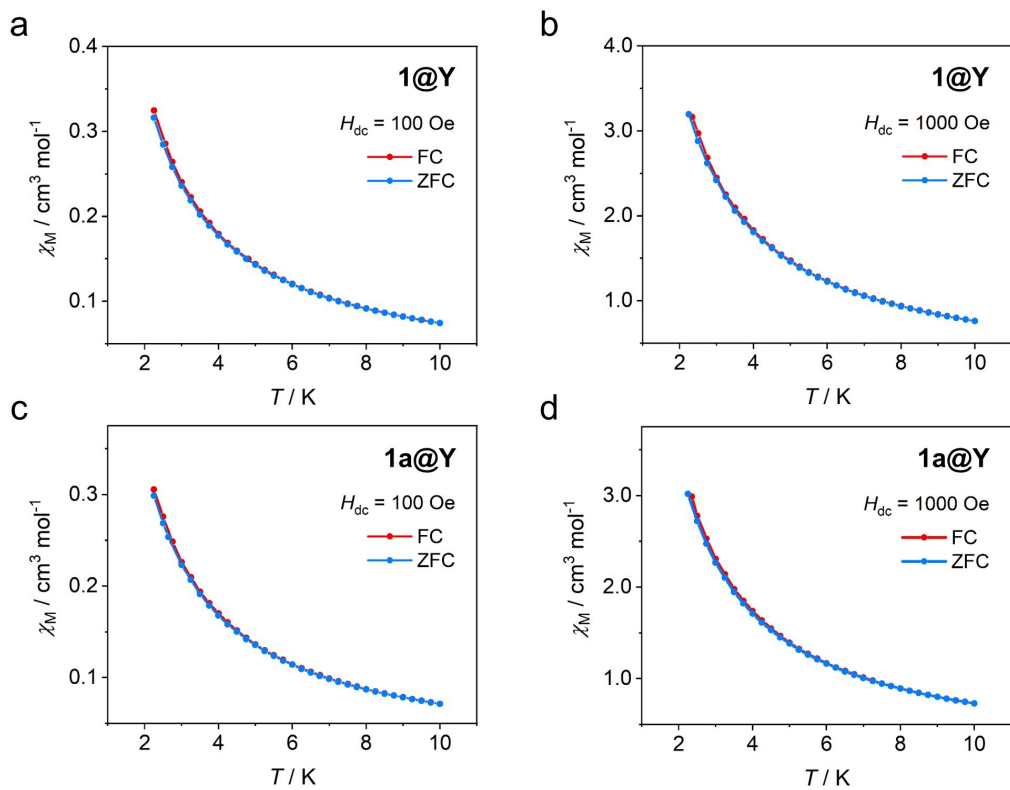


Fig. S32 FC/ZFC magnetizations at 100 Oe and 1000 Oe for **1@Y** (a, b) and **1a@Y** (c, d).

The lines are guides for the eye.

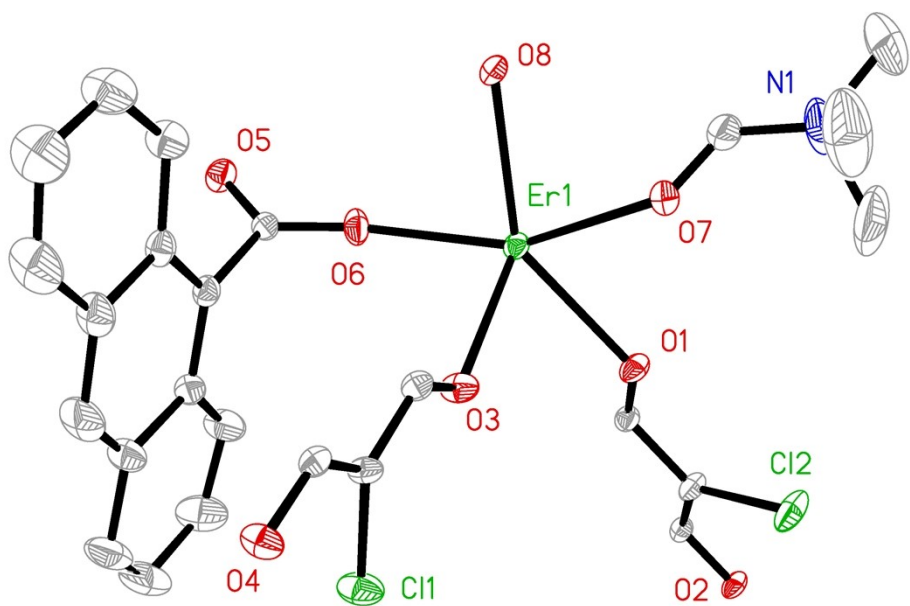


Fig. S33 The asymmetric unit of **1** showing atomic displacement parameters (ADPs).

Table S1. Crystal data and structure refinement details for **1**.

Compound	1
CCDC	2165479
Formula	C ₂₄ H ₁₈ Cl ₂ ErNO ₈
Formula weight	686.55
Temperature (K)	298(2)
Crystal colour	Brown
Wavelength (Å)	0.71073
Crystal system	Triclinic
Space group	P ¹
<i>a</i> (Å)	10.5489(3)
<i>b</i> (Å)	11.2090(3)
<i>c</i> (Å)	11.2509(3)
α (deg)	84.919(2)
β (deg)	68.177(2)
γ (deg)	82.378(2)
<i>Z</i>	2
<i>V</i> (Å ³)	1222.97(6)
ρ_{calc} (g/cm ³)	1.864
μ (mm ⁻¹)	3.700
<i>F</i> (000)	670.0
<i>R</i> _{int}	0.0376
Goodness-of-fit on <i>F</i> ²	1.030
^a <i>R</i> ₁ , ^b <i>wR</i> ₂ (<i>I</i> ≥ 2σ(<i>I</i>))	0.0290, 0.0537
^a <i>R</i> ₁ , ^b <i>wR</i> ₂ (all data)	0.0373, 0.0557
$^a R_1 = \sum F_o - F_c / \sum F_o , \quad ^b wR_2 = \left \sum w(F_o ^2 - F_c ^2) \right / \left \sum w(F_o)^2 \right ^{1/2}$	

Table S2. Symmetries and deviated values of Er(III) ion for **1**.

Shape	Symmetry	1
Octagon	D_{8h}	28.575
Heptagonal pyramid	C_{7v}	23.782
Hexagonal bipyramid	D_{6h}	13.265
Cube	O_h	8.129
Square antiprism	D_{4d}	1.262
Triangular dodecahedron	D_{2d}	2.384
Johnson gyrobifastigium J26	D_{2d}	12.409

Table S3. Magnetization relaxation fitting parameters for **1** (PPMS).

<i>T</i>	χ_s	χ_T	τ / s	α	Residual
2	1.74873	10.9073	1.60604E-4	0.11561	0.21617
2.1	1.62784	10.4805	1.54483E-4	0.12543	0.99611
2.2	1.63788	9.87197	1.43951E-4	0.103	0.37713
2.3	1.56235	9.5366	1.38902E-4	0.10814	0.91919
2.4	1.45353	9.13406	1.31175E-4	0.11572	0.47541
2.5	1.48799	8.67086	1.23064E-4	0.09177	0.43699
2.6	1.35053	8.3579	1.16573E-4	0.10883	0.75126
2.8	1.26716	7.80921	1.05975E-4	0.11004	0.52412
3	1.21204	7.27928	9.54408E-5	0.10444	0.88201
3.2	1.16861	6.71058	8.43028E-5	0.08953	0.40266
3.4	1.11791	6.32921	7.6262E-5	0.08815	0.15926
3.6	1.05988	5.92122	6.78041E-5	0.08425	0.84928
3.8	1.06164	5.60883	6.15568E-5	0.07251	0.13202
4	1.01875	5.33193	5.53811E-5	0.07166	0.50619
4.2	1.00109	4.99581	4.91746E-5	0.05681	0.40535
4.5	0.89001	4.72668	4.17232E-5	0.08016	1.63766
5	0.89061	4.12762	3.08387E-5	0.03671	1.27396
5.5	0.69647	3.8145	2.08372E-5	0.07374	0.44729
6	0.66749	3.45192	1.32215E-5	0.05179	0.46703
6.5	0.37223	3.17192	6.60859E-6	0.06945	0.35534
7	2.8832E-13	2.96331	2.33686E-6	0.1725	1.2373

Table S4. Magnetization relaxation fitting parameters for **1a** (PPMS).

<i>T</i>	χ_s	χ_T	τ / s	α	Residual
2	1.62918	9.67015	1.60233E-4	0.11578	0.12488
2.1	1.5687	9.21245	1.51664E-4	0.1106	0.16214
2.2	1.4979	8.82265	1.44662E-4	0.11102	0.14375
2.3	1.44479	8.38868	1.35796E-4	0.10422	0.29792
2.4	1.40301	8.07009	1.29673E-4	0.10087	0.27194
2.5	1.35302	7.76901	1.23469E-4	0.1009	0.13812
2.6	1.29949	7.4272	1.16133E-4	0.09829	0.21274
2.8	1.2256	6.90981	1.04783E-4	0.09421	0.12581
3	1.16549	6.4289	9.39923E-5	0.0876	0.1156
3.2	1.09634	6.03255	8.47106E-5	0.0892	0.08851
3.4	1.05235	5.64786	7.57348E-5	0.0815	0.0886
3.6	1.0016	5.31228	6.79105E-5	0.07963	0.05764
3.8	0.95908	5.03069	6.10806E-5	0.07876	0.0534
4	0.92209	4.74474	5.44099E-5	0.0729	0.07942
4.2	0.90806	4.47634	4.86099E-5	0.06079	0.27428
4.5	0.85952	4.20189	4.15158E-5	0.06623	0.16071
5	0.80764	3.70208	3.03786E-5	0.04053	0.24429
5.5	0.78941	3.35099	2.17835E-5	0.02316	0.09713
6	0.74545	3.05365	1.40095E-5	0.02383	0.04577
6.5	0.65468	2.80281	7.76676E-6	0.02804	0.0461
7	0.51562	2.58064	3.85594E-6	0.03501	0.03908

Table S5. Magnetization relaxation fitting parameters for **1@Y** (MPMS).

T	χ_s	χ_T	τ / s	α	Residual
2	0.61872	3.55877	0.00129	0.14333	0.10676
2.1	0.65768	3.37784	0.00115	0.13275	0.03378
2.2	0.65398	3.21502	0.00101	0.12586	0.03363
2.3	0.62634	3.07174	8.7959E-4	0.12879	0.02778
2.4	0.61955	2.93423	7.73911E-4	0.12219	0.02576
2.5	0.60272	2.82015	6.82028E-4	0.12361	0.02104
2.6	0.604	2.69128	6.02817E-4	0.11408	0.05568
2.8	0.58664	2.50467	4.83234E-4	0.11576	0.01607
3	0.58885	2.33473	3.95722E-4	0.1059	0.01572
3.2	0.59014	2.18766	3.2941E-4	0.09767	0.01129
3.4	0.5827	2.06224	2.76141E-4	0.09226	0.0088
3.6	0.59585	1.94656	2.3671E-4	0.07671	0.0086
3.8	0.58279	1.8468	2.00377E-4	0.07363	0.00674
4	0.55788	1.75202	1.62992E-4	0.07251	0.01174
4.2	0.52487	1.67401	1.33873E-4	0.07369	0.00958
4.4	0.54648	1.59442	1.21348E-4	0.04606	0.0041
4.8	0.22526	1.46532	5.6802E-5	0.07933	0.00693
5.2	2.54614E-13	1.35461	3.23039E-5	0.0507	0.0056
5.6	3.13189E-13	1.26372	1.6383E-5	0.21293	0.0531

Table S6. Magnetization relaxation fitting parameters for **1a@Y** (MPMS).

<i>T</i>	χ_s	χ_T	τ / s	α	Residual
2	0.72256	3.48093	0.00129	0.15378	0.72256
2.1	0.7019	3.30745	0.00113	0.15004	0.7019
2.2	0.68907	3.14807	0.001	0.14352	0.68907
2.3	0.66691	3.00857	8.84596E-4	0.14097	0.66691
2.4	0.65468	2.87753	7.88507E-4	0.13576	0.65468
2.5	0.64627	2.75871	7.04704E-4	0.13126	0.64627
2.6	0.62917	2.6512	6.29426E-4	0.12989	0.62917
2.8	0.62192	2.45395	5.15754E-4	0.1182	0.62192
3	0.63062	2.2887	4.37593E-4	0.10253	0.63062
3.2	0.59995	2.14563	3.59613E-4	0.09794	0.59995
3.4	0.60356	2.01753	3.08546E-4	0.08333	0.60356
3.6	0.57607	1.90719	2.58579E-4	0.077	0.57607
3.8	0.6157	1.80904	2.3374E-4	0.05645	0.6157
4	0.61869	1.71708	2.02671E-4	0.04096	0.61869
4.2	0.62766	1.63617	1.78206E-4	0.02082	0.62766
4.4	0.63526	1.56319	1.55941E-4	0.01172	0.63526
4.8	0.64671	1.43855	1.16781E-4	1.5957E-8	0.64671
5.2	0.67	1.33135	8.53533E-5	1.76636E-8	0.67
5.6	0.76855	1.24135	6.99081E-5	2.12719E-8	0.76855
6	0.90273	1.16158	7.17633E-5	2.55358E-8	0.90273

Table S7. Magnetization relaxation fitting parameters for **1@Y** (PPMS).

<i>T</i>	χ_s	χ_T	τ / s	α	Residual
3	1.11343	6.96954	3.62303E-4	0.23305	0.16029
3.2	1.05066	6.47932	2.89558E-4	0.23114	0.13241
3.4	0.97527	6.17528	2.43453E-4	0.24464	0.05863
3.6	0.94337	5.91621	2.05339E-4	0.24371	0.09944
3.8	0.98422	5.36412	1.58364E-4	0.20023	0.15749
4	0.98469	5.11565	1.34702E-4	0.18631	0.21574
4.2	1.03912	4.73988	1.09415E-4	0.14198	0.39974
4.4	0.98172	4.5724	9.3458E-5	0.15267	0.10247
4.6	0.97769	4.39146	7.99315E-5	0.1402	0.09661
4.8	0.96073	4.1914	6.69011E-5	0.13003	0.07793
5	0.9484	4.04549	5.64591E-5	0.12095	0.17634
5.2	0.96378	3.86693	4.70366E-5	0.09822	0.12607
5.4	0.95959	3.70455	3.84705E-5	0.07846	0.07069
5.6	0.97259	3.57984	3.14588E-5	0.0661	0.1047
5.8	0.91756	3.46358	2.45252E-5	0.07028	0.2238
6	0.87891	3.34536	1.88884E-5	0.0677	0.10841
6.2	0.8169	3.25257	1.41842E-5	0.07697	0.09653
6.4	0.89901	3.12508	1.13413E-5	0.04505	0.10424
6.6	0.90047	3.03496	8.63481E-6	0.04559	0.10866
6.8	0.33296	2.98155	4.40423E-6	0.1312	0.10141
7	9.2197E-13	2.89519	2.54513E-6	0.16327	0.0798

Table S8. Magnetization relaxation fitting parameters for **1a@Y** (PPMS).

<i>T</i>	χ_s	χ_T	τ / s	α	Residual
3	1.09423	6.74494	4.16366E-4	0.26385	0.07603
3.2	1.07187	6.17218	3.23156E-4	0.24171	0.10798
3.4	1.03368	5.77392	2.63342E-4	0.23385	0.12516
3.6	0.99438	5.41066	2.16892E-4	0.22598	0.09158
3.8	1.00066	5.09427	1.7964E-4	0.20391	0.09536
4	0.97824	4.8589	1.52666E-4	0.19634	0.08357
4.2	0.97988	4.53584	1.24883E-4	0.16833	0.09638
4.4	0.97031	4.33131	1.06126E-4	0.15508	0.10365
4.6	0.95022	4.13792	8.93218E-5	0.14458	0.07626
4.8	0.96417	3.92839	7.43285E-5	0.11576	0.08984
5	0.9378	3.78018	6.1958E-5	0.10907	0.07931
5.2	0.92596	3.61939	5.07838E-5	0.09297	0.04465
5.4	0.91507	3.47739	4.12464E-5	0.07926	0.02446
5.6	0.90827	3.35775	3.32228E-5	0.06675	0.03559
5.8	0.92106	3.22132	2.63722E-5	0.04492	0.03419
6	0.89501	3.12338	2.04769E-5	0.04234	0.04653
6.2	0.91209	3.02313	1.59994E-5	0.03176	0.02372
6.4	0.86555	2.93436	1.18878E-5	0.03827	0.02431
6.6	0.86329	2.84877	8.97213E-6	0.03796	0.01154
6.8	0.61304	2.77825	5.63503E-6	0.07679	0.06169
7	0.2848	2.71274	3.2784E-6	0.1175	0.03649

References

- [1] O. Kahn, *Molecular Magnetism*, VCH Publishers, New York, 1993.
- [2] G. M. Sheldrick, *A short history of shelx*, *Acta Crystallogr. A* 2008, **64**, 112.